The 9th International Supercritical CO_2 Energy Technologies Symposium
March 2 - 5, 2026, Pittsburgh, PA
Paper #022

Impact of Cooling Fluid on the Design and Performance of a Supercritical CO_2 Heat Exchanger for Applications in High-Temperature Heat Pumps

Dr. Emily Fricke
Postdoctoral Researcher
KTH Royal Institute of Technology
Stockholm, Sweden

Zanil Narsing
Doctoral Student
KTH Royal Institute of Technology
Stockholm, Sweden

Dr. Silvia Trevisan
Assistant Professor
KTH Royal Institute of Technology
Stockholm, Sweden

Dr. Rafael Guedez Mata
Division of Heat and Power Technology
KTH Royal Institute of Technology
Stockholm, Sweden

Emily Fricke is a postdoctoral researcher in the Division of Heat and Power Technology at KTH Royal Institute of Technology. Her research focuses on heat transfer and heat exchanger design, with the goal of advancing sustainable technologies.

Zanil Narsing is a Ph.D. student researching hybrid systems for industrial decarbonization. His research involves the validation of novel heat pumps and thermal energy storage for industrial applications to enable gradual technology adoption through reducing large upfront investment and operational risks.

Silvia Trevisan is an assistant professor in the Division of Heat and Power Technology at KTH Royal Institute of Technology. Her research focuses on the development of cost-effective thermal energy storage solutions to maximize the penetration of renewable energy while providing stability and flexibility in the energy sector.

Rafael Guedez Mata is the head of the Division of Heat and Power Technology at KTH Royal Institute of Technology. His research focuses on the development of techno-economic performance models for optimizing the design and operation of energy conversion and storage technologies, systems and power plants. Such work aims at assisting decision making for technology manufacturers, investors, project developers and operators, and policy-makers.

ABSTRACT

Heating and cooling comprise a significant area of energy consumption in industry. High-temperature heat pumps (HTHPs) equipped with thermal energy storage (TES) have the potential to meet this need and reduce industrial reliance on fossil fuels through the incorporation of renewably produced electricity, in addition to providing other opportunities to utilize waste heat and solar thermal energy. Although these heat pumps have the ability to address both heating and cooling needs, supplying heat is particularly critical, with heating accounting for about half of global energy consumption [1]. The heat sink (i.e., the refrigerant cooler) of the HTHP affects the overall system performance. In this heat exchanger, high temperature and pressure refrigerant is cooled by another fluid that is then used to charge the hot TES to meet the heating demand. This secondary refrigerant or sink fluid is a key aspect of the heat exchanger performance. CO_2 is a suitable working fluid for HTHPs, where it can operate in its supercritical state and maintain desirable heat transfer properties. This work compares the heat exchanger design and performance of a heat sink in a HTHP with CO_2 as the refrigerant for three different secondary refrigerants: thermal oil, molten salt, and air. Upper limits on the inlet pressure and temperature on the CO_2 side are 200 bar and 300 °C, respectively. These more demanding conditions make a printed circuit heat exchanger (PCHE) a desirable choice for the CO_2 cooler, which will be used for the various secondary fluids considered. The fluids present different advantages and disadvantages. Thermal oils exhibit higher boiling temperatures and superior heat transfer, but raise concerns due to flammability in addition to incurring higher costs. Molten salts also have beneficial heat transfer capabilities, with high thermal conductivities, boiling points, and heat transfer capacities, and offer the additional advantage of potentially being used as the hot TES fluid. They can be corrosive, however, and present other safety risks depending upon the specific compound used. Air, conversely, is safe, readily available, and inexpensive, but it exhibits poor heat transfer performance and results in a larger heat exchanger volume to achieve performance targets. The results suggest that, of the range of channel geometries considered, the same parameters are optimal for the three sink fluids, resulting in specific areas of 627 m^2/m^3 on the CO_2 side and 711 m^2/m^3 on the sink side. To achieve a nominally 0.5 MW capacity heat exchanger, however, the PCHE volumes are different: 0.0862 m^3 for oil, 0.0567 m^3 for molten salt, and 0.383 m^3 for air.

INTRODUCTION

There is a growing interest in developing HTHPs to provide thermal energy in industrial applications to support decarbonization. CO_2 is a safe and readily available working fluid that can be implemented in transcritical cycles to attain higher temperatures, while offering superior heat transfer capabilities (with its higher density and lower viscosity in the supercritical state). For the heat sink in the HTHP, supercritical CO_2 is cooled by a secondary working fluid. The design of this heat exchanger is critical not only from a safety perspective, but also for performance of the cycle as a whole, with the heat being removed from the CO_2 in this heat exchanger being used to meet the heating needs of the application.

Various options exist for heat exchangers operating at high temperature and pressure conditions, and it is an area of continued research as applications for such heat exchangers and manufacturing methods continue to develop. Common types identified in the literature for sCO_2 applications include printed circuit heat exchangers (PCHEs), diffusion-bonded plate and fin heat exchangers (PFHEs), and micro shell and tube heat exchangers (MSTHEs) [1]. PCHEs consist of diffusion-bonded plates with chemically etched channels, exhibiting high compactness due to the small channel size possible and robust performance at high temperatures and pressures. PFHEs are less compact and more limited in terms of the maximum pressures, with about 200 bar being suggested as the upper limit ([1], [2]). MSTHEs are simply traditional shell and tube heat exchangers, but with smaller tubes employed to increase the heat transfer surface area. While shell and tube heat exchangers are a fairly reliable and conventional technology that is also less expensive to manufacture, they can lead to higher heat exchanger volumes. This can be mitigated by using smaller tube

diameters, but other problems can then arise such as high tube-side pressure drops or blocked flow due to complications with the welding process.

A variety of channel geometries are possible for PCHEs. Channels formed from etching tend to have semi-circular cross-sections, and can be straight, zigzag, wavy, or have s-shaped or airfoil-shaped fins. PCHEs with zigzag or wavy channels offer enhanced heat transfer compared to straight channels due to their higher surface areas, but at the cost of higher pressure drops. Discontinuous fins (e.g., s-shaped or airfoil-shaped fins) can help mitigate the pressure drop, but can present concerns about the integrity of the bond between plates [3].

The secondary fluid selected is a key aspect of the heat exchanger performance. Moisseytsev and Sienicki (2014) compared to performance of water and air in cooling supercritical CO_2 at 87.3 °C and 7.6 MPa for a power cycle [4]. They found that the air-cooled PCHE would need to be 100 times larger than the water-cooled one, with the air compressor pumping power being limited to 5% of the plant output. Water, despite its benefits, must operate at high pressures to attain higher temperatures, which affects not only the design of the heat exchanger, but also the TES and associated piping. For heat pump systems providing higher temperature heat, a sink fluid that can operate at lower pressures is more desirable. Molten salt (MS), for example, is suitable for very high temperature operation and lower pressures, and several researchers have investigated the performance of sCO_2-MS heat exchangers, such as for concentrating solar power (CSP) plants. Shi et al. (2020) performed a numerical study on the performance of a supercritical CO_2-MS heat exchanger for CSP applications, with inlet conditions on both fluids ranging from 600-800 °C, with sCO_2 being the cold fluid and MS being the hot fluid [5]. They used airfoil fins on the MS side, which they found to overall be the best choice to optimize performance over straight and zigzag fins for a given pumping power. In addition to optimizing heat exchanger geometries and obtaining performance correlations for a range of inlet conditions, another area of research is the material choice for these very high temperature applications. Zhu et al. (2021) designed an MS-sCO_2 PCHE for use in CSP plants built out of a zirconium/tungsten composite, with the material being selected due to its high thermal conductivity and mechanical integrity at high temperatures [6]. The inlet conditions for the fluids were 600 °C and 20 bar for sCO_2, and 800 °C and 1 bar for MS. Comparing to a PCHE made of SS316, they found the power density using the composite to be almost 9 times greater.

For applications in HTHPs, however, high performing alloys suitable for very high temperature applications are not necessary, and stainless steel is generally sufficient in terms of mechanical properties and thermal performance. One other potential heat transfer fluid that has not been widely investigated for use with sCO_2 is thermal oil. Like MS, it can operate at higher temperatures and lower pressures. It exhibits lower maximum temperature limits than MS, though, and although operation beyond the flash point is possible, fire safety becomes a greater concern. Both thermal oil and MS represent higher-performing sink fluids, albeit with their own unique risks and drawbacks (e.g., fire safety concerns with oil, corrosiveness of MS). Air, though a poor heat transfer fluid, provides a less costly and safer option, and an interesting point for comparison.

METHODOLOGY

Fluid Properties

Representative properties for the three sink fluids are included in Table 1. Note that for thermal oil, properties of Duratherm 600 are used (with a maximum operating temperature of 315 °C) [7]. Key property data is tabulated as a function of temperature, which was used to determine material properties. For MS, HITEC is used (which has a melting temperature of 142 °C and an upper limit of 600 °C, beyond which thermal decomposition occurs) [8]. Representative property values are tabulated based upon manufacturer data, with all being given at 200 °C (note that the specific heat is valid for the liquid phase, not just at 200 °C) [9]. For the model,

correlations were taken from various sources in the literature in terms of temperature, which are included in Table 2. Properties for dry air were obtained from EES, which employs the fundamental equation of state developed by Lemmon et al. (2000) [10]. Properties for CO_2 were likewise obtained from EES, which uses the equation of state developed by Span and Wagner (1996) [11]. Note that the temperature variable in the equations in Table 2 is in °C.

Table 1: Representative properties of secondary heat transfer fluids

Fluid	Density (kg/m^3)	Viscosity (Pa-s)	Specific Heat (J/kg-K)	Thermal Conductivity (W/m-K)
Oil (20 °C)	840	0.1002	1858	0.1405
Oil (100 °C)	787	0.0053	2114	0.136
Molten salt (200 °C)	1940	7.43e-3	1562	1940
Air (20 °C, 5 bar)	5.953	1.827e-5	1013	0.02601
Air (100 °C, 5 bar)	4.665	2.195e-5	1015	0.03172

Table 2: MS correlations

Property	Correlation	Units	Temperature Range	Source
Density, ρ	$\rho = 2263 - 0.7689T$	kg/m^3	175-565 °C	[12]
Viscosity, μ	$\mu = T^{-2.104} \times 10^{5.7374}$	mPa-s	150-500 °C	[13]
Specific heat, c_p	$c_p = 1423$	(J/kg-K)	Liquid phase, <300 °C	[8]
Thermal conductivity, k	$k = -0.00064T + 0.586$	(W/m-K)	300-500 °C	[14]

Boundary Conditions

The PCHE boundary conditions are summarized in Table 3. CO_2 is assumed to enter at a temperature ranging from 250-300 °C, with a pressure of 200 bar. The CO_2 flowrate per cross-sectional area of the heat exchanger core is fixed, resulting in an inlet Reynolds number ranging from 5300-5600. The sink-side mass flowrate is varied. Each sink fluid has a fixed inlet temperature. For oil, it was assumed to be slightly elevated at 50 °C, assuming it is circulating in a loop and receives some cooling before reentering the heat exchanger without returning to atmospheric temperature. The MS temperature is higher, taken to be 150 °C so it is above the melting temperature. Meanwhile, air was assumed to be at approximately atmospheric temperature. The nominal mass flowrate of molten salt was taken to be at the upper limit of the range, as higher flowrates can help increase the power, which will be limited by the higher inlet temperature of the MS. A higher mass flowrate for air was also used to help achieve a higher heat transfer rate since air, with its lower specific heat, changes temperature relatively quickly, which causes the heat transfer to taper off despite increases in heat exchanger length. To make more effective use of the heat exchanger length and mitigate the pressure drop of the more viscous thermal oil, a lower flowrate was used.

Table 3: Boundary conditions, with range and nominal value included in parenthesis

Fluid	Inlet Temperature (°C)	Inlet Pressure (bar)	Mass flowrate per cross-sectional area (kg/m^2-s)
CO_2	250-300 (250)	200	20
Oil	50	1	5-20 (10)
MS	150	1	10-20 (20)
Air	20	5	10-20 (20)

PCHE Design and Geometric Parameter Variation

The geometry of the PCHE core, including geometric parameters for the channels, is illustrated in Figure 1. The model dimensions considered are included in Table 4.

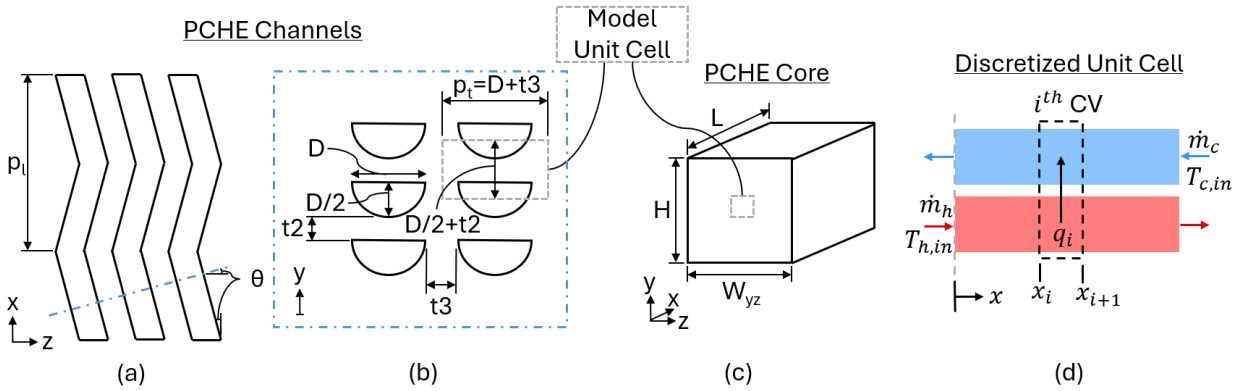

Figure 1: PCHE geometry, showing (a) the zigzag channels, (b) the channel cross-section, (c) the PCHE core, and (d) the unit cell used for modeling discretized into control volumes (CVs)

The plate thickness was selected to be a commonly available sheet thickness. The material was assumed to be SS316L, which is suitable for the upper limit on temperatures considered of 350 °C. PCHE channels typically have a semi-circular cross-sections from the etching process, with a depth ranging from about 0.1 to 2.5 mm [2]. The required wall and fin thicknesses (t2 and t3) can be determined based upon ASME Boiler and Pressure Vessel Code, Section VIII, Appendix 13-9 [15], with the application of these equations to PCHE design described by Heatric [2]. Based upon these equations and an allowable stress value of 94.1 MPa at 350 °C (from Table 1A of the ASME Boiler and Pressure Vessel Code, Section II – Materials, [16]), channel diameters and fin thicknesses can be determined. The values included in Table 4 satisfy these minimum fin and wall thicknesses required. Note that mechanical constraints on the CO_2 side prevented a channel diameter larger than 1.7 mm from being used (on both the CO_2 side and the sink side). An initial sizing was performed to choose a baseline heat exchanger length for each fluid. For all of the fluids, the nominal channel dimensions included in Table 4 were used, in addition to the nominal flow conditions from Table 3. The length was then selected to maintain a minimum pinch temperature of 10 °C for each sink fluid. This preliminary analysis resulted in baseline lengths of 0.28 m, 0.36 m, and 0.74 m for MS, air, and oil, respectively.

Table 4: PCHE geometric parameters, with nominal value included in bold

Parameter	Symbol	Value	Units
Diameter of semicircular channel	*D*	1.3, **1.5**, 1.7	mm
Plate thickness	-	1.5	mm
Wall thickness	*t2*	0.65, **0.75**, 0.85	mm
Fin thickness	*t3*	0.45, **0.55**, 0.6	mm
Transverse pitch	p_t	1.75, **2.05**, 2.3	mm
Longitudinal pitch	p_l	8	mm
Channel angle	θ	40	°
Length	*L*	0.25-75	m

Thermofluidic Model

A 1D thermofluidic model was developed to predict the performance of the heat exchanger core. The heat exchanger is assumed to operate in counterflow. The model considers a unit cell, comprising half of a channel on the CO_2 (hot) side, half of channel on the sink (cold) side, and the wall in between, as illustrated in Figure 1(b). This is then discretized along the channel length, into control volumes as shown in Figure 1(d), with the following equations applied to each control volume.

The heat transfer rate in the ith control volume (CV) q_i can be described as

$$q_i = \dot{m}\,(h_i - h_{i+1}) \tag{1}$$

where $\dot{m}$ is the mass flowrate for the unit cell and *h* is the enthalpy, evaluated at nodes i and i+1. This is applied for the CO_2 side and for the sink side when air is the sink fluid. The heat transfer rate can also be calculated as follows:

$$q_i = \dot{m}_{unit\ cell} c_{p,i} (T_i - T_{i+1}) \tag{2}$$

where $c_{p,i}$ is the specific heat (evaluated at the average properties for the CV), and *T* is the temperature. This is applied to the sink side when oil or MS is the sink fluid.

Additionally, the heat transfer rate can be calculated using the sum of thermal resistances $R_{tot,i}$ as

$$q_i = \frac{\left(T_{CO_2\ avg,i} - T_{sink\ avg,i}\right)}{R_{tot,i}} \tag{3}$$

where $T_{CO_2\ avg,i}$ and $T_{sink\ avg,i}$ denote the average CO_2 and sink temperatures in the ith CV, respectively. $R_{tot,i}$ is given by

$$R_{tot,i} = R_{conv\ CO_2,i} + R_{cond} + R_{conv\ sink,i} \tag{4}$$

with R_{conv} and R_{cond} denoting the convective and conductive resistances, respectively. The conductive resistance is assumed to be constant for all CVs, and is evaluated as

$$R_{cond} = \frac{t2}{k_{wall} A_{wall,i}} \tag{5}$$

Or, for the case where different channel diameters on the two fluid sides result in different

values of t2, the following equation is used:

$$R_{cond} = 2 * \left(k_{wall} A_{wall,i} \left(\frac{1}{t2_{CO2}} + \frac{1}{t2_{sink}} \right) \right)^{-1} \quad (6)$$

The thermal conductivity of the wall material k_{wall} is evaluated at the average of the two fluid inlet temperatures. The heat transfer area for conductivity in the ith CV $A_{wall,i}$ is simply the product of the unit cell width (p_t) and the effective length of the ith CV ($L_{channel,CV}=L_{CV}/cos(\theta)$). Convective thermal resistance is given by

$$R_{conv} = \frac{1}{htc_i A_{conv,i}} \quad (7)$$

where htc_i is the convective heat transfer coefficient for the ith CV and $A_{conv,i}$ is the convective heat transfer area. $A_{conv,i}$ is simply

$$A_{conv,i} = \frac{1}{2}(D + \pi D) L_{channel,CV} \quad (8)$$

The heat transfer coefficient is given by

$$htc_i = \frac{Nu_i k_i}{D_h} \quad (9)$$

where k_i is the thermal conductivity of the fluid, evaluated at the average of the fluid temperature at the inlet and outlet of the control volume and D_h is the hydraulic diameter, defined as

$$D_h = \frac{4A}{P} \quad (10)$$

where A is the cross-sectional area and P is the wetted perimeter. The Reynolds number Re is key in determining the Nusselt number, and is evaluated as a function of density ρ, velocity V, D_h, and dynamic viscosity μ as follows:

$$Re = \frac{\rho V D_h}{\mu} \quad (11)$$

The Nusselt number Nu and friction factor f are evaluated using correlations. For flow on the CO_2 side, the correlations developed by Saeed et al. (2020) for a zigzag PCHE in which supercritical CO_2 is cooled by water are implemented [17].

$$Nu_{sCO_2} = 0.475 Re^{0.61} Pr^{0.17} \quad (12)$$

$$f_{sCO_2} = 0.13 Re^{-0.044} \quad (13)$$

where Pr is the Prandtl number. Note that these correlations were developed for $3000 \leq Re \leq 60000$ and $2.0 \leq Pr \leq 13$. A limitation of this correlation (and many others available in the literature) is its specificity for the fluids, fluids conditions, and geometries over which they were developed. The channel geometry is similar to that considered here (zigzag channels with a 40° bend angle). Zilio et al. (2024) investigated the applicability of different Nusselt number correlations for PCHEs with straight and zigzag channels, including Eq. (12), finding it to have reasonable accuracy in predicting experimental data (below 6% total mean error) [18].

For the sink fluid, the correlations developed by Hesselgreaves (2001) for fully developed flow with $Re \leq 2300$ in straight, semi-circular channels were implemented for laminar flow (which are applicable to various fluids) [19]:

$$Nu = 4.089 \quad (14)$$

$$f = \frac{15.78}{Re} \tag{15}$$

For higher Reynolds number flow on the sink side (above 2300), the Nusselt number can be calculated via the Gnielinski correlation (relevant for $0.5 < Pr < 2000$ and $2300 < Re < 5\ x\ 10^6$) while the friction factor can be calculated using the correlation from Petukhov (1970) for smooth flow in a duct (valid for fully developed flow with $3000 < Re < 5\ x\ 10^6$), both tabulated by Nellis and Klein (2009) [20].

$$Nu = \frac{\frac{f}{8}(Re - 1000)Pr}{1 + 12.7\left(Pr^{\frac{2}{3}} - 1\right)\sqrt{\frac{f}{8}}} \tag{16}$$

$$f = (0.790\ln(Re) - 1.64)^{-2} \tag{17}$$

Note that the friction factor correlation was applied despite being slightly out of range when Reynolds number is between 2300 and 3000.

For each fluid stream, the pressure drop across a CV can be calculated as

$$\Delta P_i = f_i \frac{L_{channel,CV}}{D_h} \frac{1}{2} \rho_i V_i^2 \tag{18}$$

The total pressure drop is then the sum of the pressure drops in all the control volumes along the heat exchanger length.

It is worth noting that both the oil and MS are very low Reynolds flow, with inlet Reynolds numbers below 20. Despite the tendency of correlations for straight channels to underestimate heat transfer and pressure drop in zigzag channels, these correlations were applied rather than selecting other correlations and extending them far below their range of validity. Also, these correlations are applicable to different fluids, and for fluids like oil, it is difficult to find existing correlations.

RESULTS AND DISCUSSION

Parametric Study for Different Fluids

For the different sink fluids, the performance of the PCHE core was evaluated for the different combinations of channel geometry options. Five different channel geometry cases were considered, henceforth referred to using the shorthand notation below:

1. 1.3/1.3: the case in which both fluids have a 1.3 mm channel diameter and the corresponding wall thickness and transverse pitch
2. 1.5/1.5: the case in which both fluids have a 1.5 mm channel diameter and the corresponding wall thickness and transverse pitch
3. 1.7/1.7: the case in which both fluids have a 1.7 mm channel diameter and the corresponding wall thickness and transverse pitch
4. 1.3/1.5: the case in which the CO_2 channels have a 1.3 mm diameter and the sink channels have a 1.5 mm diameter, with the transverse pitch corresponding to the pitch tabulated for 1.3 mm diameter channels
5. 1.5/1.7: the case in which the CO_2 channels have a 1.5 mm diameter and the sink channels have a 1.7 mm diameter, with the transverse pitch corresponding to the pitch tabulated for 1.5 mm diameter channels

Note that for the 1.3/1.5 and 1.5/1.7 cases, using the pitch corresponding to the higher pressure CO_2 side still allows the necessary structural integrity to be maintained, since the sink side is at much lower pressure.

Figure 2 illustrates the impact of variation in channel geometry on heat exchanger performance for oil as the sink fluid. Two key competing metrics are used to assess performance: power density and sink-side pressure drop. While heat transfer performance

can be enhanced by smaller flow passages, this comes at the cost of higher pressure drop. For the various geometries, the power density ranges from 3 to 8.3 MW/m^3, and the sink pressure drop from 0.44 to 19.0 kPa over the range of sink flow rates considered (from 5 to 20 kg/m^2-s). The sink pressure drop is lowest for the 1.5/1.7 case. This is because it has the largest hydraulic diameter for the sink, which helps mitigate the pressure drop, while having a slightly higher surface area on the CO_2 side than the case where both fluids have 1.7 mm channels, which enhances the heat transfer and results in higher temperature oil with a lower viscosity. While smaller channels sizes lead to higher specific areas and, hence, higher power densities, there is very little variation in the power density. Shifting from the 1.3/1.3 case to the 1.3/1.5 case or from 1.5/1.5 to 1.5/1.7 generally results in a very slight increase in power density, which can be explained by the fact that the transverse pitch is maintained at a constant value while the sink channel diameter increases, resulting in a slight increase in heat transfer area that counteracts the increased hydraulic diameter. That said, the percent difference in power density is below 0.1% for both cases. The maximum values for power densities are observed for the 1.3/1.5 case. However, the percent increase in power density from the 1.5/1.7 case to the 1.3/1.5 case is only 1.24% on average, while the average percent increase in sink pressure drop is 35%. Similar trends are seen with an inlet temperature of 300 °C for CO_2, with average percent increases when going from case 1.5/1.7 to case 1.3/1.5 in power density and sink pressure drop of 1.26% and 35%, respectively.

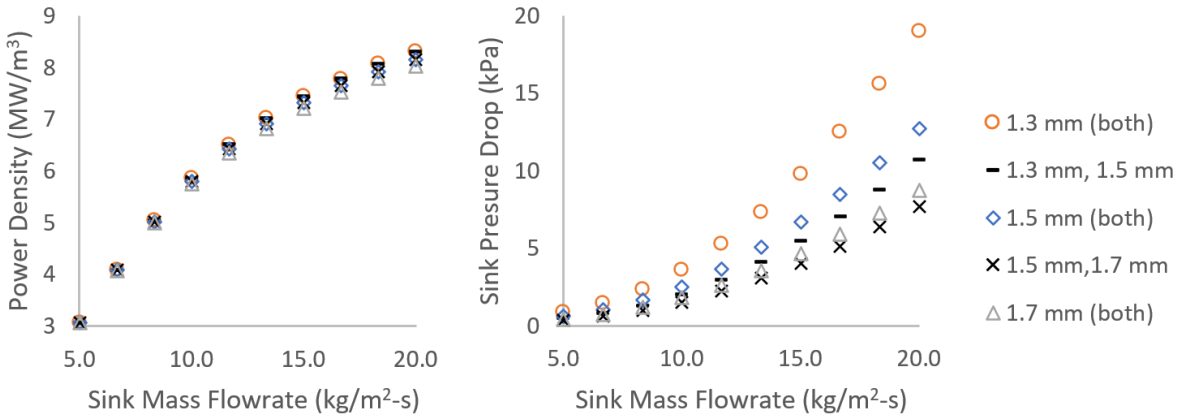

Figure 2: Parametric data for oil with a CO_2 inlet temperature of 250 °C and a heat exchanger core length of 0.74 m.

The parametric data for MS as the sink fluid is shown in Figure 3. The power density is slightly higher compared to the oil-cooled heat exchanger, ranging from about 5 to 9 MW/m^3. The predicted pressure drops are much lower, with values from about 0.6 to 4.0 kPa. This can be ascribed in part to the shorter core length. As before, the optimal sizing to minimize pressure drop is 1.5/1.7, while the sizing with the highest power density is 1.3/1.5. Changing from 1.5/1.7 to 1.3/1.5 results in an average increase in power density of 0.91% and an average increase in pressure drop in 39%. Likewise, for a CO_2 inlet temperature of 300 °C, this geometry change is accompanied by average percent increases in power density and pressure drop of 0.96% and 38%, respectively. Hence. The 1.5/1.7 sizing can be deemed the superior option.

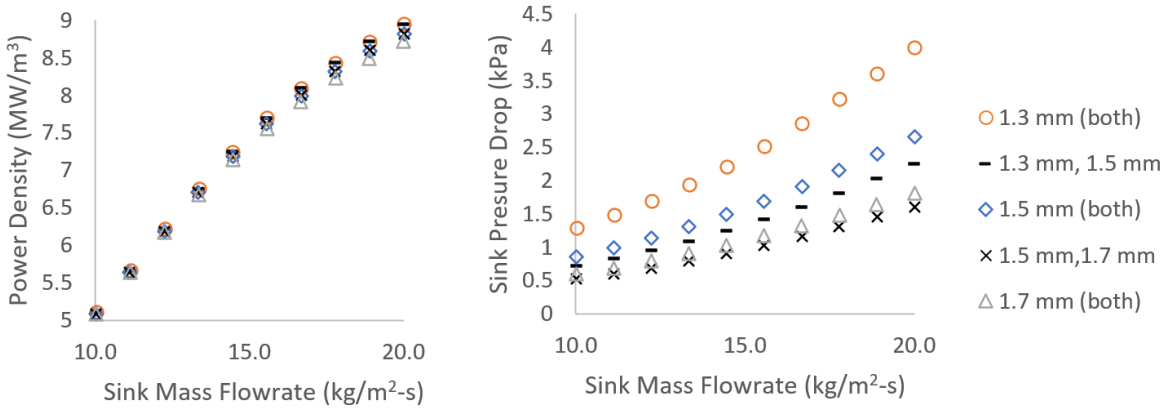

Figure 3: Parametric data for MS with a CO_2 inlet temperature of 250 °C and a heat exchanger core length of 0.28 m.

Figure 4 shows the impact of channel geometry variation with air as the sink fluid. Of note is the higher power densities than those observed with oil and MS, ranging from 6.5 to 12.6 MW/m^3. The pressure drop is also much higher, with minimum and maximum values of 14.7 and 132 kPa. Although the same trend as with the other fluids is observed for pressure drop in terms of which geometries have higher pressure drops, here the smaller sink-side channels result in the highest power densities (i.e., 1.3/1.3 has a higher power density than 1.3/1.5, and 1.5/1.5 has a higher power density than 1.5/1.7). This can be explained by the effects of the smaller channel size on the heat transfer coefficient outweighing the impact of the slight surface area increase for air. Considering the best choice in terms of mitigating pressure drop, 1.5/1.7, changing to the geometry with the next lowest pressure drop (1.7/1.7) results in a 22% average increase in pressure drop. Changing to the geometry with the best heat transfer performance (1.3/1.3) results in a 193% average increase in pressure drop. Meanwhile, the power density is only enhanced by an average of 1.3% when the geometry is changed from 1.5/1.7 to 1.3/1.3. Similarly, at a CO_2 inlet temperature of 300 °C, shifting from 1.5/1.7 to 1.3/1.3 results in a 1.44% average increase in power density but a 196% average increase in pressure drop. Thus, 1.5/1.7 is the most desirable choice.

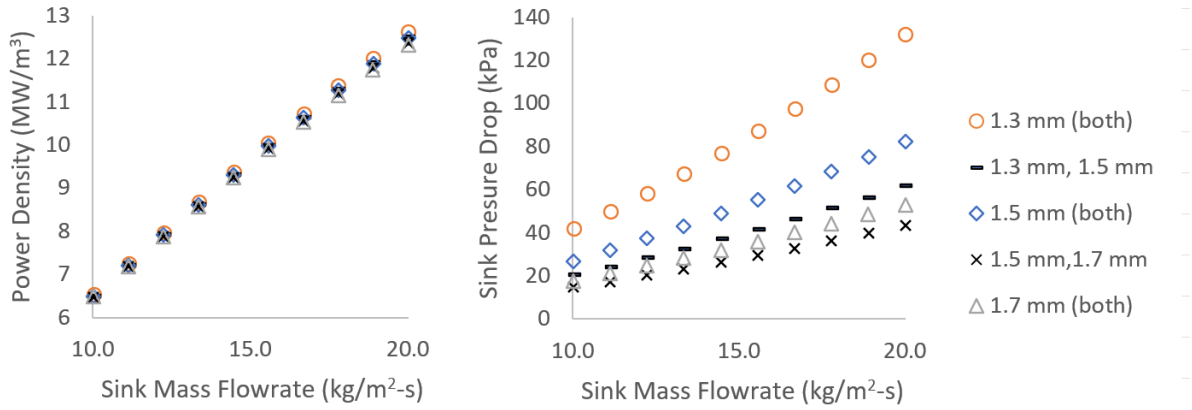

Figure 4: Parametric data for air with a CO_2 inlet temperature of 250 °C and a heat exchanger core length of 0.36 m.

The same trend was observed across the fluids, with a significant increase in pressure drop occurring when channel size was reduced, accompanied by minor enhancements of the power density. One caveat is that for the oil and MS cases where the channel sizes were different between the CO and the sink, the case with the larger sink channel actually had a slightly higher power density than for the case with two channels of the same size. For all the fluids, a geometry of 1.5 mm semicircular channels on the CO_2 side and 1.7 mm semicircular channels on the sink side seems optimal. This geometry results in a heat exchanger with a

specific surface area of 627 m^2/m^3 on the CO_2 side and 711 m^2/m^3 on the sink side.

Using the nominal flowrates considered for the different fluids (10 kg/m^2-s for oil and 20 kg/m^2-s for MS and air), to obtain a nominally 0.5 MW/m^3 capacity for a CO_2 inlet temperature of 250-300 °C, heat exchanger core volumes of 0.0686-0.0862 m^3 for oil (corresponding to a width/height of 0.30-0.34 m), 0.0386-0.0567 m^3 for MS (corresponding to a width/height of 0.37-0.45 m), and 0.0334-0.0404 m^3 for air (corresponding to a width/height of 0.30-0.34) are required. The outlet temperature of the CO_2 is an important parameter to keep in mind, as it impacts the rest of the heat pump cycle. For oil, MS, and air, the CO_2 outlet temperature ranges are 110-114 deg C, 161-164 deg C, 107-114 deg C and respectively. Note that the higher CO_2 outlet temperature observed with MS is due to the higher inlet temperature of MS compared to the other sink fluids.

Another key aspect to note is that the air-cooled heat exchanger is assumed to have the lowest inlet temperature of the three sink fluids considered, which helps enhance the heat transfer. Additionally, using air comes at the cost increased pumping power. Pumping power is proportional to the product of the volumetric flowrate and the pressure drop. In addition to having a pressure drop that is an order of magnitude higher than the other fluids, air has a density that 2-3 orders of magnitude smaller, resulting in a much higher pumping power. At the nominal condition considered, the pumping power per cross sectional area ranges from 146-156 kW/m^2 (assuming a pump with 100% efficiency), in comparison to 16.8-18.7 W/m^2 for oil and 13.1-15.0 W/m^2 for molten salt. Hence, although the conditions considered predict as smaller air-cooled PCHE, a lower air flow rate should be considered to achieve more realistically acceptable values for pumping power.

Applying the nominal volumetric flowrates for oil and MS, Figure 5 plots the variation in power density and pumping power versus heat exchanger core length for a CO_2 inlet temperature of 250 °C. Results for air are also included, but at a reduced flow rate of 2 kg/m^2-s to obtain lower pumping powers more on par with the other sink fluids. Here, it is clear that using air as the sink fluid while limiting the flowrate to mitigate pressure drop will require a much larger volume than the other fluids. To achieve the nominally 0.5 MW capacity heat exchanger, and assuming the core length is the 0.36 m considered previously, a volume of 0.383 m^3 is required, resulting in cross-sectional core dimensions of 1.03 x 1.03 m (or, for a CO_2 inlet temperature of 300 °C, a volume of 0.314 m^3 and cross-sectional dimensions of 0.93 x 0.93 m). At the nominal length of 0.36 m, the pumping power per cross-sectional area for air ranges from 131-153 W/m^2. As the oil and MS heat exchangers require smaller cross-sectional areas, this will also lead to an increase in overall pumping power relative to the other sink fluids since pumping power in Figure 5 is plotted per cross-sectional area. Considering the cross-sectional area ranges, the actual pumping power is projected to be 1.56-2.2 W for oil, 1.81-3.0 W for MS, and 133-140 W for air.

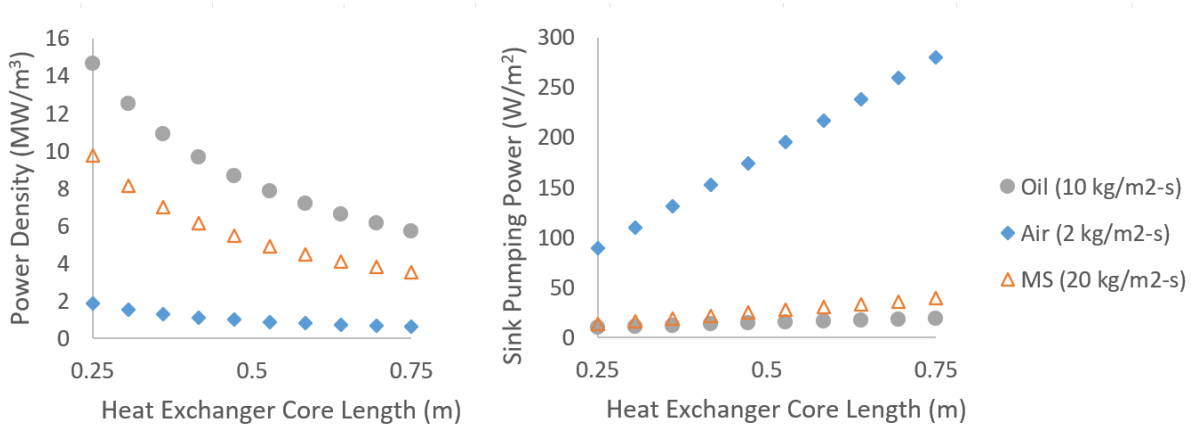

Figure 5: PCHE performance with a CO_2 inlet temperature of 250 °C for oil, MS, and air at different core lengths.

The heat transfer performance when using the different sink fluids can also be considered by examining the average heat transfer coefficients. For all of the sink fluids, over the various heat exchanger lengths considered in Figure 5 (with a CO_2 inlet temperature of 250 °C), the average heat transfer coefficient on the CO_2 side ranged from 4307-4352 W/m^2-K. For oil, MS, and air, meanwhile, the ranges are 517-524 W/m^2-K, 1817-1823 W/m^2-K, and 157.5-161.3 W/m^2-K respectively. Hence, purely from the perspective of heat transfer capability, MS is the superior choice, followed by thermal oil, then by air.

Of note in Figure 5 is also the fact that as heat exchanger length increases, there is a diminishing benefit in terms of increase in heat transfer. This is observed for all fluids, but the trend is most dramatic for air. This is because the air, due to its lower specific heat, approaches the temperature of the CO_2 stream as it flows through the heat exchanger length more readily than the other fluids.

Performance of an MS-cooled Higher-temperature PCHE

As noted previously, MS is suitable for use at higher temperatures. Consider the case where CO_2 enters the heat sink at a temperature of 450 °C and a pressure of 200 bar. Applying the nominal boundary conditions and the optimal geometry (case 1.5/1.7), Figure 6 shows the variation in power density and pressure drop with length. Note that using this geometry, the mechanical integrity of the PCHE is still maintained. To maintain a pinch temperature below 10 °C, a length of at least 0.56 m is required. At this length, the outlet temperature of the MS is 410 °C, enabling higher temperature process heat to be supplied. The corresponding power density and pressure drop are 13.4 MW/m^3 and 2.2 kPa, respectively. To supply 0.5 MW of heating, the heat exchanger volume is 0.0374 m^3, resulting in cross-sectional dimensions of 0.26 x 0.26 m.

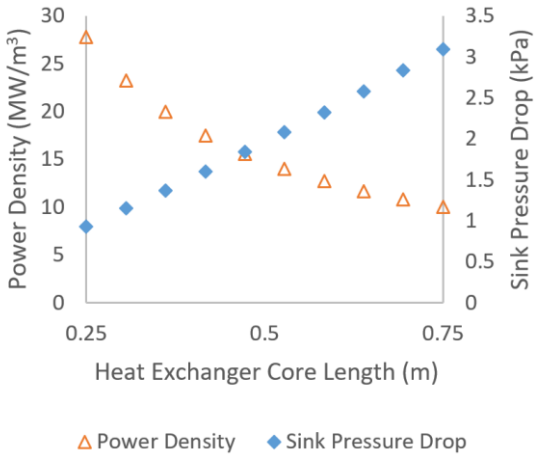

Figure 6: PCHE performance with a CO_2 inlet temperature of 450 °C for MS at different core lengths.

CONCLUSIONS

The performance of a counterflow printed circuit type heat exchanger in which supercritical CO_2 is cooled by three different sink fluids was considered. One commonality across the fluids was findings regarding the optimal geometry of the channels. For the different channel diameters considered, the optimal geometry had 1.5 mm and 1.7 mm diameters of the semicircular channels for CO_2 and the sink fluid, respectively. For the standard plate thickness of 1.5 mm considered, larger diameter channels were not feasible while maintaining the necessary mechanical integrity at the 200 bar CO_2 pressure, and smaller channels resulted in only marginal improvements in heat transfer and high pressure drops. Due to its poor heat transfer properties, air is a less desirable choice of sink fluid. At the nominal conditions and the reduced flow rate considered, it requires a heat exchanger volume about 8 times that needed for MS and 5 times that needed for thermal oil to achieve the same thermal capacity,

with a pumping power that is still two orders of magnitude larger than for the other sink fluids. To make the use of air feasible, a hybrid design with sink-side flow passages more suitable for air would have to be considered (incorporating larger hydraulic diameters to mitigate the pressure drop). MS performs the best in terms of compactness, but other key limitations are related to the limit on CO_2 outlet temperature due to the higher melting point of MS, as well as the expense, corrosiveness, and potential safety concerns raised by the fluid. MS is already often used to exchange heat with CO_2 in higher temperature applications such as CSP power cycles due to its superior properties and suitability for such conditions, but it presents a potential option for use in lower temperature applications in HTHPS as considered here. Thermal oil still allows for a reasonably compact heat exchanger just under twice the size of the MS heat exchanger. It has not been widely investigated in CO_2 cooling, but has potential for exploration to allow for higher temperatures to be reached at lower pressures (as does MS). The main drawbacks with thermal oil are the cost and fire safety concerns. In the future, a PCHE design informed by this work is planned to be manufactured for testing as part of a heat pump system, with thermal oil as the cooling fluid.

REFERENCES

[1] Chai, L., & Tassou, S. A. (2023). Recent Progress on High Temperature and High Pressure Heat Exchangers for Supercritical CO_2 Power Generation and Conversion Systems. *Heat Transfer Engineering, 44*(21–22), 1950–1968. https://doi.org/10.1080/01457632.2022.2164683.

[2] Le Pierres, R., Southall, D., & Osborne, S. (2011). Impact of Mechanical Design Issues on Printed Circuit Heat Exchangers. *Proceedings of the SCO_2 Power Cycle Symposium,* Boulder, CO, USA.

[3] Kwon, J. S., Son, S., Heo, J. Y., & Lee, J. I. (2020). Compact heat exchangers for supercritical CO_2 power cycle application. *Energy Conversion and Management, 209.* https://doi.org/10.1016/j.enconman.2020.112666.

[4] Moisseytsev, A., & Sienicki, J. J. (2014). Investigation of Dry Air Cooling Option for an s-CO_2 Cycle. *Proceedings of the SCO_2 Power Cycle Symposium,* Pittsburgh, PA, USA.

[5] Shi, H.-Y., Li, M.-J., Wang, W.-Q., Qiu, Y., & Tao, W.-Q. (2020). Heat transfer and friction of molten salt and supercritical CO2 flowing in an airfoil channel of a printed circuit heat exchanger. *International Journal of Heat and Mass Transfer, 150.* https://doi.org/10.1016/j.ijheatmasstransfer.2019.119006.

[6] Zhu, Q., Tan, X., Barari, B., Caccia, M., Strayer, A. R., Pishahang, M., Sandhage, K. H., & Henry, A. (2021). Design of a 2 MW ZrC/W-based molten-salt-to-sCO2 PCHE for concentrated solar power. *Applied Energy, 300.* https://doi.org/10.1016/j.apenergy.2021.117313.

[7] Duratherm. *Duratherm 600 Technical Data Sheet.* Retrieved September 18, 2025 from https://durathermfluids.com/pdf/productdata/heattransfer/duratherm-600.pdf.

[8] Parida, D. R., & Basu, S. (2023). On the specific heat capacity of HITEC-salt nanocomposites for concentrated solar power applications. *RSC Advances, 13,* 5496-5508. https://doi.org/10.1039/D2RA07384F.

[9] Coastal Chemical Co., L.L.C. HITEC Heat Transfer Salt. Retrieved on September 18, 2025 from http://www.coal2nuclear.com/MSR%20-%20HITEC%20Heat%20Transfer%20Salt.pdf .

[10] Lemmon, E.W., Jacobsen, R.T., Penoncello, S.G., & Friend, D. (2000). Thermodynamic Properties of Air and Mixtures of Nitrogen, Argon, and Oxygen from 60 to 2000K at Pressures to 2000 MPa. *Journal of Physical and Chemical Reference Data, 29*(3).

[11] Span, R., & Wagner W. (1996). A New Equation of State for Carbon Dioxide Covering the Fluid Region from the Triple-Point Temperature to 1100 K at Pressures up to 800 MPa. *Journal of Physical and Chemical Reference Data, 25*(6).

[12] Jung, C., & Spenke, C. (2023). Volumetric Determination of Densities of Molten Salts for CSP Applications. *Proceedings of SolarPACES 2023, the 29th International Conference on Concentrating Solar Power, Thermal, and Chemical Energy Systems,* Sydney, Australia. https://doi.org/10.52825/solarpaces.v2i.914.

[13] Xiao, X., Zhang, G., Ding, Y., & Wen, D. (2019). Rheological Characteristics of Molten Salt Seeded with Al_2O_3 Nanopowder and Graphene for Concentrated Solar Power. *Energies, 12*(3), 467. https://doi.org/10.3390/en12030467.

[14] Wu, Y.-T., Chen, C., Liu, B., & Ma, C.-F. (2012). Investigation on forced convective heat transfer of molten salts in circular tubes. *International Communications in Heat and Mass Transfer, 39*(10), 1550-1555. https://doi.org/10.1016/j.icheatmasstransfer.2012.09.002.

[15] American Society of Mechanical Engineers. (2023). *2023 ASME Boiler and Pressure Vessel Code, Section VIII, Division 1.* American Society of Mechanical Engineers (ASME).

[16] American Society of Mechanical Engineers. (2023). *2023 ASME Boiler and Pressure Vessel Code, Section II - Materials.* American Society of Mechanical Engineers (ASME).

[17] Saeed, M., Berrouk, A. S., Siddiqui, M. S., Awais, A. A. (2020). Numerical investigation of thermal and hydraulic characteristics of sCO_2-water printed circuit heat exchangers with zigzag channels. *Energy Conversion and Management, 224.* https://doi.org/10.1016/j.enconman.2020.113375.

[18] Zilio, G., Moura, M.R., dos Santos, F.J., Possamai, T.S., & Mortean, M.V.V. (2024). Nusselt number analysis of printed circuit heat exchangers with straight and zigzag channels. *International Journal of Heat and Fluid Flow, 107.* https://doi.org/10.1016/j.ijheatfluidflow.2024.109395.

[19] Hesselgreaves, J. E. (2001). *Compact Heat Exchangers: Selection, Design and Operation.* Elsevier.

[20] Nellis, G. F., & Klein, S. A. (2009). *Heat transfer*. Cambridge University Press.

ACKNOWLEDGEMENTS

This research was funded by CETPartnership, the Clean Energy Transition Partnership under the 2023 joint call for research proposals, co-funded by the European Commission (GA N°101069750) and with the funding organizations detailed on https://cetpartnership.eu/funding-agencies-and-call-modules. The project has received support from the Swedish Energy Agency, Scottish Enterprise, and the CDTI.